Journal of Applied Mathematics and Physics, 2025, 13(8), 2621-2644
https://www.scirp.org/journal/jamp
ISSN Online: 2327-4379
ISSN Print: 2327-4352

# Dynamic Analysis of a Class of Intraguild Predation Systems with Time Delay

**Yawei Xue, Xiaolin Lin, Danfeng Pang, Wangwang Liu**

School of Mathematics and Data Science, Shaanxi University of Science and Technology, Xi'an, China
Email: linxiaolin@sust.edu.cn

**How to cite this paper:** Xue, Y.W., Lin, X.L., Pang, D.F. and Liu, W.W. (2025) Dynamic Analysis of a Class of Intraguild Predation Systems with Time Delay. *Journal of Applied Mathematics and Physics*, **13**, 2621-2644.
https://doi.org/10.4236/jamp.2025.138149

**Received:** July 24, 2025
**Accepted:** August 17, 2025
**Published:** August 20, 2025

Copyright © 2025 by author(s) and Scientific Research Publishing Inc.
This work is licensed under the Creative Commons Attribution International License (CC BY 4.0).
http://creativecommons.org/licenses/by/4.0/
Open Access

## Abstract

Based on the niche theory, a class of delayed intraguild predation systems integrating Holling type I and type II functional response functions is constructed. Firstly, the existence conditions of the positive equilibrium point of the system are clarified. Secondly, the dynamic behavior of the system is analyzed from two aspects: in the absence of time delay, the local stability of the positive equilibrium point of the system is analyzed by using the Hurwitz criterion. In the presence of time delay, with the gestation delay of the predator population as the bifurcation parameter, the existence of Hopf bifurcation near the positive equilibrium point of the system is explored, and the properties of Hopf bifurcation are analyzed by means of the center manifold theorem and normal form theory. Finally, the correctness of the theoretical derivation is verified by numerical simulation.

## Keywords

Intraguild Predation, Stability, Hopf Bifurcation, Delay

## 1. Introduction

Ecosystems are the foundation for the survival and development of life on Earth, encompassing the intricate interactions between organisms and between organisms and their environment. In the fields of ecology and mathematical ecology, predation systems are key tools for depicting the population relationships between predators and prey. Traditional predation systems primarily focus on the dynamic balance between the two, predicting quantitative changes through population growth equations. Classic systems such as the Lotka-Volterra model have established a quantitative framework for predatory behaviors, exploring the impact of predatory interactions on population structure, stability, and ecosystem functions [1]. However, predation phenomena in real-world ecosystems are far more com-

plex than the assumptions of such systems. Especially when involving population hierarchy, behavioral characteristics, and temporal factors, there is a need to further expand and refine these systems. Numerous organisms in an ecosystem are interdependent and mutually restrictive, maintaining the stability of ecological balance. If this balance is disrupted, it will trigger a chain reaction, profoundly affecting the structure and function of the ecosystem, and thereby impacting biodiversity and human survival and development. Therefore, in-depth research on its dynamic characteristics is of great significance.

The niche theory, as a core concept in ecology, defines the unique position and role of an organism or population within an ecosystem. Traditional ecology holds that species at the same trophic level mainly compete, while species at different trophic levels primarily exhibit predation. However, in natural ecological communities, species relationships are actually more complex; species at the same trophic level often have a dual relationship of both competition and predation [2] [3].

In 1992, Polis and Holt [3] first proposed the concept of Intraguild Predation (IGP), and constructed a classic IGP system in 1997 [4]. This system includes three populations: a shared food resource (P), an intraguild prey (G), and an intraguild predator (M). In the system, the IGP predator M not only preys on the IGP prey G but also feeds on the shared resource P; there is a predator-prey relationship between the IGP prey G and the shared resource P; and the IGP predator M and the IGP prey G compete for the shared resource P. The IGP system effectively depicts the complex ecological phenomenon where two species both compete for the same shared resource and prey on each other. For example, in freshwater ecosystems, bluegill sunfish and some insects both feed on plankton, and bluegill sunfish prey on these insects; in desert ecosystems, spiders and scorpions both prey on insects, and they have a dual relationship of competition and predator-prey [5]. Such systems, integrating predation and competition, provide a new perspective for in-depth analysis of interactions across multiple trophic levels in food chains, and are of great significance for maintaining ecological diversity and conducting wildlife management.

In 1995, Rosenheim *et al.* [6] concluded from experiments that IGP systems have indirect effects on population trophic levels; in 2010, Arim and Marquet [7] pointed out that IGP systems are widespread in nature, and there may be certain deviations in expected results for different populations. They also argued that the determining factor for the persistent coexistence of IGP systems is the characteristics of the biological populations. In 2013, Kang and Wedekin [8] proposed two types of intraguild predation (IGP) systems, and their research results showed that: 1) Both types of IGP systems can have multiple attractors with complex dynamic patterns; 2) Only IGP systems with monophagous predators can have both boundary attractors and internal attractors, meaning whether a species goes extinct or all three species coexist depends on initial conditions; 3) IGP systems with omnivorous predators are prone to the coexistence of all three species. In 2021, Bai *et al.* [9] proposed a class of intraguild predation systems where the basal food

source exhibits logistic growth with a strong Allee effect. Their research results indicated that the intraguild predation food web system displays rich and complex dynamic behaviors, and the strong Allee effect in the basal prey not only increases the risk of extinction for the basal prey but also raises the risk of extinction for the IGP prey or IGP predator.

Delay phenomena are widely prevalent in natural systems. In multidisciplinary fields such as ecology, physics, and biology, delay differential equations are more capable of depicting the dynamic processes of systems in a way that aligns with reality compared to conventional equations [10]. For biological systems, the occurrence of time delays can be traced back to factors such as biological growth and development, reproductive cycles, and fluctuations in environmental factors, which significantly affect the dynamic evolution of populations. Introducing the dimension of time delay into the construction of predator-prey models can more accurately restore the real functioning mechanisms of ecosystems. Existing studies often incorporate the ecological process where "the energy obtained by predators through feeding is not immediately converted into reproductive output" into the model framework in the form of time delay through Holling-type functional responses [11] [12]. The existence of time delay may not only change the dynamic behavior patterns of the system but also potentially induce system instability. Based on this, conducting research on predator models with time delay holds crucial theoretical value for analyzing the laws of dynamic changes and the mechanisms maintaining stability in ecosystems. Therefore, it is of great significance to consider time delay in intraguild predation (IGP) ecosystems. The inclusion of time delay significantly increases the dynamic complexity of IGP systems, enabling them to more truly reflect the evolutionary laws of ecosystems. Taking desert spider communities as an example, the predatory regulation of wolf spiders (dominant predators) on the population surge of jumping spiders (inferior predators) is delayed due to time lags in individual development cycles and environmental adaptation [5]; in freshwater fish communities, the population growth of bass after preying on sunfish is delayed due to time lags such as gestation and larval growth. IGP systems with time delay can accurately depict the lag effects generated by ecosystems due to response delays and reveal nonlinear oscillations, coexistence of multiple steady states, and potential critical transition phenomena in population quantities [13]-[15].

In summary, in-depth analysis of the dynamic behaviors of time-delayed intraguild predation ecosystems helps clarify their internal regulatory mechanisms, provides key theoretical basis for biodiversity conservation, invasive species control, and sustainable management of ecological resources, and lays the foundation for formulating scientific and effective management strategies to cope with changes in ecosystem structure and function. Notably, unlike previous studies that either employed a single functional response or neglected time delay in the IGP framework, this model innovatively integrates both Holling type I and type II functional responses with a time delay, thereby offering a more comprehensive perspective on the complex dynamics of such systems.

## 2. Model Construction

In 1992, Holt and Polis [3] [4] applied the classic Lotka-Volterra predator-prey system to intraguild predation relationships. They denoted the common prey, intraguild prey, and intraguild predator as $P(t)$, $G(t)$, and $M(t)$ respectively, and established the following classic intraguild predation system:

$$\begin{cases} \dfrac{\mathrm{d}P}{\mathrm{d}t} = P\left[r\left(1-\dfrac{P}{K}\right)-a_g G - a_m M\right], \\ \dfrac{\mathrm{d}G}{\mathrm{d}t} = G\left[b_g a_g P - c_m M - d_g\right], \\ \dfrac{\mathrm{d}M}{\mathrm{d}t} = M\left[b_m a_m P + \rho c_m G - d_m\right], \end{cases}$$

where $r$ represents the intrinsic growth rate of the common prey, $K$ represents the maximum environmental carrying capacity of the common prey, $a_g$ and $a_m$ respectively represent the predation rates of the intraguild prey and the intraguild predator on the common prey, $c_m$ represents the predation rate of the intraguild predator on the intraguild prey, $b_g$ and $b_m$ respectively represent the conversion rates of the intraguild prey and the intraguild predator for the common prey, $\rho$ represents the conversion rate of the intraguild predator for the intraguild prey, and $d_g$ and $d_m$ respectively represent the natural mortality rates of the intraguild prey and the intraguild predator.

In the classic IGP system, the growth of the common prey follows the logistic growth law. The IG prey only feeds on the common prey, and the IG predator feeds on both the common prey and the IG prey. The predation of the common prey by the intraguild prey and the intraguild predator both follow the Holling type I functional response function. This choice aligns with findings by Murdoch [16], who demonstrated that Holling type I is typical for filter feeders and passive predators (such as many invertebrates) consuming abundant, low-level prey, consistent with the common prey and intraguild prey interactions described here. In actual ecosystems, there may also be other situations regarding the interaction relationship between the IG prey and the IG predator for the shared resource and the interaction relationship between the IG prey and the IG predator themselves.

In 2025, Li *et al.* [12], considering the gestation delay of the predator, constructed a type of delayed predation system with cannibalism, fear effect, and Holling type II functional response:

$$\begin{cases} \dfrac{\mathrm{d}x(t)}{\mathrm{d}t} = \dfrac{ax(t)}{1+by(t)} - cx^2(t) - \dfrac{\varphi_1 x(t) y(t)}{x(t)+m}, \\ \dfrac{\mathrm{d}y(t)}{\mathrm{d}t} = \dfrac{\varphi_2 x(t-\tau) y(t-\tau)}{x(t-\tau)+m} + (r-d) y(t) - \dfrac{\sigma y^2(t)}{y(t)+n}. \end{cases}$$

The research results show that the delayed gestation of the predator population has a significant impact on population dynamics. An appropriate gestation delay of the predator may lead to the occurrence of Hopf bifurcation near the positive equilibrium point of the system. The research achievements provide a new per-

spective for understanding the population interactions in ecosystems and highlight the crucial role of the delayed gestation of the predator population in terms of ecosystem stability and population dynamics.

Considering that common prey are mostly low-level organisms, intraguild prey are mostly invertebrates, and IG predators are mostly vertebrates or large carnivores. In 1959, Holling [17] originally proposed type II responses to describe predators with limited handling time, a characteristic of vertebrate predators (like the IG predators here) that must process each prey item, supporting our use of type II for IG predator-IG prey interactions. By constructing a system where both the growth of the common prey and the IG prey follow the logistic growth law, the interaction relationship between the IG prey and the IG predator for the shared resource adopts the Holling type I functional response function, while the interaction relationship between the IG predator and the IG prey adopts the Holling type II functional response function. Referring to the method of considering time delay in the Holling type II functional response in reference [14], we consider that there is a time delay in the predation of the common prey by the predator. To sum up, the following mathematical system is established:

$$\begin{cases} \dfrac{\mathrm{d}P(t)}{\mathrm{d}t} = r_p P(t)\left(1-\dfrac{P(t)}{K_p}\right) - a_g P(t)G(t) - a_m P(t)M(t), \\ \dfrac{\mathrm{d}G(t)}{\mathrm{d}t} = r_g G(t)\left(1-\dfrac{G(t)}{K_g}\right) + b_g a_g P(t)G(t) - \dfrac{c_m G(t)M(t)}{1+dG(t)}, \\ \dfrac{\mathrm{d}M(t)}{\mathrm{d}t} = b_m a_m P(t)M(t) + \rho\dfrac{c_m G(t-\tau)M(t-\tau)}{1+dG(t-\tau)} - d_m M(t), \end{cases} \tag{1}$$

where $r_p$ and $r_g$ represent the intrinsic growth rates of the common prey and the intraguild prey respectively; $K_p$ and $K_g$ represent the maximum environmental carrying capacities of the common prey and the intraguild prey respectively; $a_g$ and $a_m$ represent the predation rates of the intraguild prey and the intraguild predator on the common prey respectively; $b_g$ and $b_m$ represent the conversion rates of the intraguild prey and the intraguild predator for the common prey respectively; $d$ represents the semi - satiety and constant of the predator; $c_m$ represents the maximum predation rate $\rho$ represents the conversion rate of the intraguild predator for the intraguild prey; $d_m$ represents the natural mortality rate of the intraguild predator. $\tau$ is the predation time delay of the predator population, which is a constant independent of time $t$, and $\tau \geq 0$.

To simplify the system, first, the following dimensionless transformation is performed on system (1). Let

$$x = \frac{P}{K_p}, y = \frac{G}{K_g}, z = \frac{a_m M}{r_p}, t = r_p t, a = \frac{a_g K_g}{r_p}, \alpha = \frac{r_g}{r_p}, \beta = \frac{K_p b_m a_m}{r_p},$$

$$\gamma = \frac{b_g a_g K_p}{r_g}, b_1 = \frac{c_m r_p}{r_g a_m}, b_2 = \frac{\rho c_m K_g}{K_p b_m a_m}, c = dK_g, \mu = \frac{1}{K_p b_m a_m} d_m.$$

Thus, system (1) is transformed into the following system:

$$\begin{cases} \dfrac{\mathrm{d}x(t)}{\mathrm{d}t} = x(t)\big(1-x(t)-ay(t)-z(t)\big), \\ \dfrac{\mathrm{d}y(t)}{\mathrm{d}t} = \alpha y(t)\left(1-y(t)+\gamma x(t)-\dfrac{b_1 z(t)}{1+cy(t)}\right), \\ \dfrac{\mathrm{d}z(t)}{\mathrm{d}t} = \beta z(t)\big(x(t)-\mu\big)+\dfrac{\beta b_2 y(t-\tau)z(t-\tau)}{1+cy(t-\tau)}. \end{cases} \tag{2}$$

In the following, the analysis will mainly focus on the dynamical behaviors of system (2).

## 3. Existence and Dynamical Analysis of Positive Equilibrium Points

### 3.1. Existence of Positive Equilibrium Points

Within the scope of this study, we exclude the scenario of biological extinction, and the core of the research focuses on the relevant situations of the positive equilibrium point of the system. The following is a detailed analysis of the existence of the positive equilibrium point of system (2).

If system (2) has a positive equilibrium point, it should satisfy:

$$\begin{cases} x_*\big(1-x_*-ay_*-z_*\big)=0, \\ \alpha y_*\left(1-y_*+\gamma x_*-\dfrac{b_1 z_*}{1+cy_*}\right)=0, \\ \beta z_*\big(x_*-\mu\big)+\dfrac{\beta b_2 y_* z_*}{1+cy_*}=0. \end{cases} \tag{3}$$

First, from the third equation of the system of Equations (3), we can obtain:

$$x_* = \mu - \frac{b_2 y_*}{1+cy_*}.$$

Assume $\mu > \dfrac{b_2 y_*}{1+cy_*}$, then $x_* > 0$. Next, substituting $x_* = \mu - \dfrac{b_2 y_*}{1+cy_*}$ into the first equation of the system of Equations (3), we can obtain:

$$z_* = 1-x_*-\alpha y_* = 1-\mu+\frac{b_2 y_*}{1+cy_*}-\alpha y_*.$$

Assume $1+\dfrac{b_2 y_*}{1+cy_*}-\alpha y_* > \mu$, then $z_* > 0$. Finally, substituting $x_* = \mu - \dfrac{b_2 y_*}{1+cy_*}$ and $z_* = 1-x_*-\alpha y_*$ into the second equation of the system of Equations (3), we can obtain:

$$y^3 - \sigma_1 y^2 - \sigma_2 y - \sigma_3 = 0, \tag{4}$$

where

$$\sigma_1 = -\frac{c^2-2c+c^2\gamma\mu-\gamma b_2 c+ab_2 c}{c^2},$$

$$\sigma_2 = -\frac{2c-1+2c\gamma\mu-\gamma b_2+b_1\mu c-b_1 b_2-b_1 c+ab_2}{c^2},$$

$$\sigma_3 = -\frac{1+\gamma\mu-b_1+b_1\mu}{c^2}.$$

By descartes' rule of signs, it can be known that when $\sigma_3 < 0$, Equation (4) has at least one positive real root. The following condition is given:

$$(H_1)\ \sigma_3 < 0 \text{ and } \frac{b_2 y_*}{1+cy_*} < \mu < 1+\frac{b_2 y_*}{1+cy_*} - \alpha y_*.$$

If condition $(H_1)$ holds, then system (2) has at least one positive equilibrium point.

In summary, the existence of the positive equilibrium point of system (2) can be summarized as the following theorem:

**Theorem 1.** If condition $(H_1)$ holds, then system (2) has at least one positive equilibrium point, where

$$(H_1)\ \sigma_3 < 0 \text{ and } \frac{b_2 y_*}{1+cy_*} < \mu < 1+\frac{b_2 y_*}{1+cy_*} - \alpha y_*.$$

### 3.2. Dynamical Analysis of Positive Equilibrium Points

This section focuses on analyzing the dynamical behavior of the positive equilibrium point of the system. Since the stability analysis of the positive equilibrium point in the case without time delay is the basis for studying the Hopf bifurcation of the time-delay system, the system will be discussed in depth for the two cases of $\tau = 0$ and $\tau > 0$, respectively.

Perform a coordinate transformation on system (2) by letting $x(t) = x(t) - x_*$, $y(t) = y(t) - y_*$, $z(t) = z(t) - z_*$; for convenience, we still denote them as $x(t)$, $y(t)$, $z(t)$. The resulting linearized system is

$$\begin{cases} \dfrac{\mathrm{d}x(t)}{\mathrm{d}t} = a_{11}x(t) + a_{12}y(t) + a_{13}z(t), \\ \dfrac{\mathrm{d}y(t)}{\mathrm{d}t} = a_{21}x(t) + a_{22}y(t) + a_{23}z(t), \\ \dfrac{\mathrm{d}z(t)}{\mathrm{d}t} = a_{31}x(t) + a_{33}z(t) + a_{34}y(t-\tau) + a_{35}z(t-\tau). \end{cases} \tag{5}$$

where

$$a_{11} = 2 - x_* - \alpha y_* - z_*, a_{12} = -\alpha x_*, a_{13} = -z_*, a_{21} = \gamma\alpha y_*,$$

$$a_{22} = \alpha - 2\alpha y_* - \frac{b_1\alpha z(1+cy_*) - b_1\alpha c z y_*}{(1-cy_*)^2}, a_{23} = -\frac{b_1\alpha(1+cy_*) - b_1\alpha c z y_*}{(1-cy_*)^2},$$

$$a_{31} = \beta z_*, a_{33} = \beta x_*, a_{34} = \frac{\beta b_2 z_*}{(1+cy_*)^2}, a_{35} = \frac{\beta b_2 y_*}{1+cy_*}.$$

The characteristic equation of system (5) is:

$$\begin{vmatrix} \lambda - a_{11} & -a_{12} & -a_{13} \\ -a_{21} & \lambda - a_{22} & -a_{23} \\ -a_{31} & -a_{34}\mathrm{e}^{-\lambda\tau} & \lambda - \left(a_{33} + a_{35}\mathrm{e}^{-\lambda\tau}\right) \end{vmatrix} = 0,$$

which can be rewritten in the following form:

$$\lambda^3 + p_1\lambda^2 + p_2\lambda + p_3 + \left(q_1\lambda^2 + q_2\lambda + q_3\right)e^{-\lambda\tau} = 0, \tag{6}$$

where

$$p_1 = -\left(a_{11} + a_{22} + a_{33}\right),\ p_2 = a_{11}a_{22} + a_{11}a_{33} + a_{22}a_{33} - a_{13}a_{31} - a_{12}a_{21},$$

$$p_3 = -a_{11}a_{22}a_{31} - a_{12}a_{23}a_{31} + a_{13}a_{31}a_{22} + a_{12}a_{21}a_{33},$$

$$q_1 = -a_{35},\ q_2 = a_{11}a_{35} + a_{22}a_{35} - a_{23}a_{34},$$

$$q_3 = -a_{11}a_{22}a_{35} - a_{13}a_{21}a_{34} + a_{11}a_{23}a_{34} + a_{12}a_{21}a_{35}.$$

(1) When $\tau = 0$, the system has no time delay, and the characteristic Equation (6) becomes:

$$\lambda^3 + \left(p_1 + q_1\right)\lambda^2 + \left(p_2 + q_2\right)\lambda + p_3 + q_3 = 0. \tag{7}$$

The following conditions are given:

$\left(H_2\right)$ $p_1 + q_1 > 0,\ p_3 + q_3 > 0$ and $\left(p_1 + q_1\right)\left(p_2 + q_2\right) > p_3 + q_3$.

According to the Hurwitz criterion, if condition $\left(H_2\right)$ holds, all the characteristic roots of the characteristic Equation (7) have negative real parts. Therefore, if condition $\left(H_2\right)$ holds, the positive equilibrium point $E_*\left(x_*, y_*, z_*\right)$ of system (2) is locally asymptotically stable.

(2) When $\tau > 0$, let the imaginary number $\lambda = i\omega\left(\omega > 0\right)$ be a root of the characteristic Equation (6). Substituting $\lambda = i\omega$ into the characteristic Equation (6) gives

$$\left(i\omega\right)^3 + p_1\left(i\omega\right)^2 + p_2\left(i\omega\right) + p_3 + \left[q_1\left(i\omega\right)^2 + q_2\left(i\omega\right) + q_3\right]\left(\cos\omega\tau - i\sin\omega\tau\right) = 0, \tag{8}$$

By separating the real and imaginary parts of Equation (8), the following transcendental equation is obtained:

$$\begin{cases} q_2\omega\cos\omega\tau + \left(q_1\omega^2 - q_3\right)\sin\omega\tau = \omega^3 - p_2\omega, \\ \left(q_3 - q_1\omega^2\right)\cos\omega\tau + q_2\omega\sin\omega\tau = p_1\omega^2 - p_3. \end{cases} \tag{9}$$

By squaring both sides of the first and second equations of Equation (10) and then adding them together, we obtain the following algebraic equation regarding $\omega$:

$$\omega^6 + \left(p_1^2 - q_1^2 - 2p_2\right)\omega^4 + \left(p_2^2 - q_2^2 - 2p_1p_3 + 2q_1q_3\right)\omega^2 + p_3^2 - q_3^2 = 0, \tag{10}$$

Let $v = \omega^2$, and substitute it into the algebraic Equation (10) to obtain

$$v^3 + m_1v^2 + m_2v + m_3 = 0, \tag{11}$$

where

$$m_1 = p_1^2 - q_1^2 - 2p_2,\ m_2 = p_2^2 - q_2^2 - 2p_1p_3 + 2q_1q_3,\ m_3 = p_3^2 - q_3^2.$$

Let

$$f\left(v\right) = v^3 + m_1v^2 + m_2v + m_3. \tag{12}$$

It can be observed that the zeros of the function $f\left(v\right)$ coincide with the roots of Equation (11). Suppose there exists a positive real root for Equation (11). With respect to the number of roots of the aforesaid Equation (11), it holds that for a positive real root $v$, there must exist a corresponding pair of pure imaginary numbers which are roots of Equation (6), denoted as $\pm i\omega = \pm i\sqrt{v}$. The condition

$(H_3)$ for Equation (11) to have a positive real root is:

1) If $m_3 < 0$, then the Equation (11) has at least one positive root;

2) If $m_3 \geq 0$, $m_1^2 - 3m_2 > 0$, $v_* > 0$ and $f(v_*) = 0$, then the Equation (11) has a unique positive root;

3) If $m_3 \geq 0$, $m_1^2 - 3m_2 > 0$, $v_* > 0$ and $f(v_*) < 0$, then the Equation (11) has two positive roots;

where

$$v_* = \frac{-m_1 + \sqrt{m_1^2 - 3m_2}}{3}.$$

Equation (11) has at most three positive real roots. Suppose Equation (11) has three positive real roots, which are represented by $v_1, v_2$ and $v_3$ respectively. Then Equation (6) has roots $i\omega_j = i\sqrt{v_j}$ $(j = 1,2,3)$.

Substituting $\omega_j$ into Equation (9) yields:

$$\tau_k^j = \frac{1}{\omega_j}\arccos\frac{(q_2 - p_1q_1)\omega_j^4 + (p_1q_3 + p_3q_1 - p_2q_2)\omega_j^2 - p_3q_3}{q_1^2\omega_j^4 + (q_2^2 - 2q_1q_3)\omega_j^2 + q_3^2} + \frac{2k\pi}{\omega_j},$$

where $j = 1,2,3$, $k = 0,1,2,3,\cdots$. Letting $\tau_0 = \min\{\tau_k^j, j = 1,2,3; k = 0,1,2,3,\cdots\}$, it can be known that when $\tau = \tau_0$, Equation (6) will have a pair of purely imaginary roots $\pm i\omega_0$, and all other roots will have non-zero real parts.

Next, we will verify the transverse condition for the occurrence of Hopf bifurcation.

First, we take the derivative of both sides of Equation (6) with respect to $\tau$, and we can obtain:

$$\left[3\lambda^2 + 2p_1\lambda + p_2 + (2q_1\lambda + q_2)e^{-\lambda\tau} - (q_1\lambda^2 + q_2\lambda + q_3)\tau e^{-\lambda\tau}\right]\frac{d\lambda}{d\tau}$$
$$= (q_1\lambda^2 + q_2\lambda + q_3)\lambda e^{-\lambda\tau}.$$

Therefore,

$$\left(\frac{d\lambda}{d\tau}\right)^{-1} = \frac{3\lambda^2 + 2p_1\lambda + p_2 + (2q_1\lambda + q_2)e^{-\lambda\tau} - (q_1\lambda^2 + q_2\lambda + q_3)\tau e^{-\lambda\tau}}{(q_1\lambda^2 + q_2\lambda + q_3)\lambda e^{-\lambda\tau}}$$
$$= -\frac{3\lambda^2 + 2p_1\lambda + p_2}{\lambda(\lambda^3 + p_1\lambda^2 + p_2\lambda + p_3)} + \frac{2q_1\lambda + q_2}{(q_1\lambda^2 + q_2\lambda + q_3)\lambda} - \frac{\tau}{\lambda},$$

From Equation (9), we can deduce that [1]

$$(p_1\omega^2 - p_3)^2 + (\omega^3 - p_2\omega)^2 = q_2^2\omega^2 + (q_1\omega^2 - q_3)^2.$$

Hence,

$$\mathrm{Re}\left[\left(\frac{d\lambda(\tau)}{d\tau}\right)^{-1}\right]_{\tau=\tau_0}$$
$$= \mathrm{Re}\left(-\frac{3\lambda^2 + 2p_1\lambda + p_2}{\lambda(\lambda^3 + p_1\lambda^2 + p_2\lambda + p_3)} + \frac{2q_1\lambda + q_2}{(q_1\lambda^2 + q_2\lambda + q_3)\lambda} - \frac{\tau}{\lambda}\right)_{\lambda=i\omega_0}$$
$$= \frac{3\omega_0^4 + 2(p_1^2 - q_1^2 - 2p_2)\omega_0^2 + (p_2^2 - q_2^2 - 2p_1p_3 + 2q_1q_3)}{(p_1\omega_0^2 - p_3)^2 + (\omega_0^3 - p_2\omega_0)^2}.$$

From $v_0 = \omega_0^2$, it follows that when $f(v)$ satisfies condition $(H_4)$, we have $\mathrm{Re}\left(\frac{\mathrm{d}\lambda}{\mathrm{d}\tau}\right)_{\tau=\tau_0} \neq 0$, where

$$(H_4)\ f'(v_0) \neq 0.$$

At this point, the transversality condition is satisfied, indicating that system (2) undergoes a Hopf bifurcation at the positive equilibrium point $E_*(x_*, y_*, z_*)$.

To sum up, the main conclusions regarding the local asymptotic stability of system (2) at the positive equilibrium point and the existence of Hopf bifurcation in its vicinity can be drawn as follows:

**Theorem 2.** When $\tau = 0$, if condition $(H_2)$ holds, then the positive equilibrium point $E_*(x_*, y_*, z_*)$ of system (2) is locally asymptotically stable, where,

$$(H_2)\ p_1 + q_1 > 0,\ p_3 + q_3 > 0, (p_1 + q_1)(p_2 + q_2) > p_3 + q_3.$$

**Theorem 3.** When $\tau > 0$, if conditions $(H_2)$, $(H_3)$, and $(H_4)$ hold, then the following conclusions can be drawn:

(1) If $\tau \in [0, \tau_0)$, then the positive equilibrium point $E_*(x_*, y_*, z_*)$ of system (2) is locally asymptotically stable.

(2) If $\tau > \tau_0$, then the positive equilibrium point $E_*(x_*, y_*, z_*)$ of system (2) is unstable.

(3) If $\tau = \tau_0$, then system (2) undergoes a Hopf bifurcation at the positive equilibrium point $E_*(x_*, y_*, z_*)$.

## 4. Direction and Stability of Hopf Bifurcation

In this section, the direction of the bifurcation solution and the stability of the positive equilibrium point $E_*(x_*, y_*, z_*)$ of system (2) will be explained by using the center manifold theorem and the normal form theory.

Expanding system (2) in Taylor series at the positive equilibrium point $E_*(x_*, y_*, z_*)$ yields:

$$\begin{cases} \dfrac{\mathrm{d}x(t)}{\mathrm{d}t} = a_{11}x(t) + a_{12}y(t) + a_{13}z(t) + f_1(t), \\ \dfrac{\mathrm{d}y(t)}{\mathrm{d}t} = a_{21}x(t) + a_{22}y(t) + a_{23}z(t) + f_2(t), \\ \dfrac{\mathrm{d}z(t)}{\mathrm{d}t} = a_{31}x(t) + a_{33}z(t) + a_{34}y(t-\tau) + a_{35}z(t-\tau) + f_3(t), \end{cases} \tag{13}$$

where

$$f_1(t) = a_{14}x^2(t) + a_{15}x(t)y(t) + a_{16}x(t)z(t),$$

$$f_2(t) = a_{24}x(t)y(t) + a_{25}y^2(t) + a_{26}x(t)z(t),$$

$$f_3(t) = a_{36}x(t)z(t) + a_{37}y^2(t-\tau) + a_{38}y(t-\tau)z(t-\tau),$$

with

$$a_{14} = -1,\ a_{15} = -\alpha,\ a_{16} = -1,$$

$$a_{24}=-\gamma\alpha,\ a_{25}=-\alpha+\frac{c\alpha b_1 z_*}{\left(1+cy_*\right)^3},\ a_{26}=-\frac{\alpha b_1}{\left(1+cy_*\right)^2},$$

$$a_{36}=\beta,\ a_{37}=-\frac{\beta b_2 c z_*}{\left(1+cy_*\right)^3},\ a_{38}=-\frac{\beta b_2}{\left(1+cy_*\right)^2}.$$

By the transformation $t\to t/\tau$, the time delay is normalized, and by letting $\tau=\tau_0+\mu$, $\mu\in\mathbb{R}$, Equation (12) can be rewritten as

$$\begin{cases}\dfrac{\mathrm{d}x(t)}{\mathrm{d}t}=(\tau_0+\mu)\left[a_{11}x(t)+a_{12}y(t)+a_{13}z(t)+f_1(t)\right],\\ \dfrac{\mathrm{d}y(t)}{\mathrm{d}t}=(\tau_0+\mu)\left[a_{21}x(t)+a_{22}y(t)+a_{23}z(t)+f_2(t)\right],\\ \dfrac{\mathrm{d}z(t)}{\mathrm{d}t}=(\tau_0+\mu)\left[a_{31}x(t)+a_{33}z(t)+a_{34}y(t-1)+a_{35}z(t-1)+f_3(t)\right].\end{cases}\tag{14}$$

It is known that the phase space is $C=C\left(\left[-1,0\right],\mathbb{R}^3\right)$, and from the previous analysis, it is understood that $\mu=0$ is the bifurcation value at which system (13) undergoes a Hopf bifurcation [1].

Define

$$L_\mu(\phi)=(\tau_0+\mu)\begin{pmatrix}a_{11}&a_{12}&a_{13}\\a_{21}&a_{22}&a_{23}\\a_{31}&0&a_{33}\end{pmatrix}\begin{pmatrix}\phi_1(0)\\\phi_2(0)\\\phi_3(0)\end{pmatrix}+(\tau_0+\mu)\begin{pmatrix}0&0&0\\0&0&0\\0&a_{34}&a_{35}\end{pmatrix}\begin{pmatrix}\phi_1(-1)\\\phi_2(-1)\\\phi_3(-1)\end{pmatrix},$$

and

$$F(\mu,u_t)=(\tau_0+\mu)\begin{pmatrix}a_{14}\phi_1^2(0)+a_{15}\phi_1(0)\phi_2(0)+a_{16}\phi_1(0)\phi_3(0)\\a_{24}\phi_1(0)\phi_2(0)+a_{25}\phi_2^2(0)+a_{26}\phi_2(0)\phi_3(0)\\a_{36}\phi_1(0)\phi_3(0)+a_{37}\phi_2^2(-1)+a_{38}\phi_2(-1)\phi_3(-1)\end{pmatrix},$$

where $L_\mu:C\left[-1,0\right]\to\mathbb{R}^3$ is a bounded linear operator and $F:\mathbb{R}\times C\left[-1,0\right]\to\mathbb{R}^3$ is continuously differentiable, then

$$\frac{\mathrm{d}u_t}{\mathrm{d}t}=L_\mu(u_t)+F(\mu,u_t),$$

with $u_t(\theta)=u(t+\theta)$, $\theta\in\left[-1,0\right]$.

By the Riesz representation theorem, there exists a bounded variation function $\eta(\mu,\theta)$ (for $\theta\in\left[-1,0\right]$) satisfying

$$L_\mu(\phi)=\int_{-1}^{0}\mathrm{d}\eta(\mu,\theta)\phi(\theta).$$

In practice, $\eta(\mu,\theta)$ can be explicitly chosen as

$$\eta(\mu,\theta)=(\tau_0+\mu)\begin{pmatrix}a_{11}&a_{12}&a_{13}\\a_{21}&a_{22}&a_{23}\\a_{31}&0&a_{33}\end{pmatrix}\delta(\theta)-(\tau_0+\mu)\begin{pmatrix}0&0&0\\0&0&0\\0&a_{34}&a_{35}\end{pmatrix}\delta(\theta+1),$$

where

$$\delta(\theta)=\begin{cases}1, & \theta=0,\\0, & \theta\neq 0.\end{cases}$$

For $\phi \in C\left(\left[-1,0\right],\mathbb{R}^3\right)$, define that

$$G(\mu)\phi(\theta)=\begin{cases}\dfrac{\mathrm{d}\phi(\theta)}{\mathrm{d}\theta}, & \theta\in[-1,0),\\ \int_{-1}^{0}\mathrm{d}\eta(\mu,\theta)\phi(\theta), & \theta=0,\end{cases}$$

and

$$R(\mu)\phi(\theta)=\begin{cases}0, & \theta\in[-1,0),\\ F(\mu,\phi), & \theta=0,\end{cases}$$

Thus, system (14) is corresponding to

$$\frac{\mathrm{d}u_t}{\mathrm{d}t}=G(\mu)u_t+R(\mu)u_t. \tag{15}$$

For $\psi \in C\left(\left[0,1\right],\left(\mathbb{R}^3\right)^*\right)$, define the conjugate operator $G^*$ of $G$ as follows:

$$G^*\psi(s)=\begin{cases}-\dfrac{\mathrm{d}\psi(s)}{\mathrm{d}s}, & s\in(0,1],\\ \int_{-1}^{0}\mathrm{d}\eta^{\mathrm{T}}(\mu,t)\psi(-t), & s=0,\end{cases}$$

Next, for $\phi \in C\left(\left[-1,0\right],\mathbb{R}^3\right)$ and $\psi \in C\left(\left[0,1\right],\left(\mathbb{R}^3\right)^*\right)$, define the bilinear inner product as

$$\left\langle\psi(s),\phi(\theta)\right\rangle=\bar{\psi}(0)\phi(0)-\int_{-1}^{0}\int_{0}^{\theta}\bar{\psi}(\xi-\theta)\mathrm{d}\eta(\theta)\phi(\xi)\mathrm{d}\xi,$$

where $\eta(\theta)=\eta(0,\theta)$. This inner product satisfies the adjoint property: $\left\langle\psi,G\phi\right\rangle=\left\langle G^*\psi,\phi\right\rangle$.

The following is about the calculation of eigenvectors. Here, let $G=G(0)$ and its conjugate operator $G^*=G^*(0)$. Suppose the eigenvalues of $G$ are $\pm i\omega_0\tau_0$. it is straightforward to verify that these are also eigenvalues of $G^*$. Calculate the eigenvectors corresponding to the eigenvalues $i\omega_0\tau_0$ and $-i\omega_0\tau_0$ with respect to matrices $G$ and $G^*$, respectively, where each eigenvalue corresponds to a different matrix.

Let $q(\theta)=(1,q_1,q_2)^{\mathrm{T}}\mathrm{e}^{i\omega_0\tau_0\theta}$ denote the eigenvector of $G$ corresponding to $i\omega_0\tau_0$. By definition, we derive:

$$q(0)=(1,q_1,q_2)^{\mathrm{T}},\ q(-1)=q(0)\mathrm{e}^{-i\omega_0\tau_0},$$

From the definition of $G(0)$, we further deduce that

$$\begin{aligned}G(0)\phi(0)&=\int_{-1}^{0}\mathrm{d}\eta(0,\theta)\phi(\theta)\\&=\tau_0\begin{pmatrix}a_{11}&a_{12}&a_{13}\\a_{21}&a_{22}&a_{23}\\a_{31}&0&a_{33}\end{pmatrix}\phi(0)+\tau_0\begin{pmatrix}0&0&0\\0&0&0\\0&a_{34}&a_{35}\end{pmatrix}\phi(-1),\end{aligned}$$

Next, from the fact that $G(0)q(0)=i\omega_0\tau_0q(0)$, we can deduce that

$$q_1=\frac{a_{23}(a_{11}-i\omega_0)-a_{13}a_{21}}{a_{13}(a_{22}-i\omega_0)-a_{12}a_{23}},\ q_2=-\frac{a_{11}-i\omega_0+q_1a_{12}}{a_{13}}.$$

Similarly, let $q^*(s)=D\left(1,q_1^*,q_2^*\right)\mathrm{e}^{i\omega_0\tau_0 s}$ be the eigenvector of graph $G^*$ with respect to the eigenvalue $-i\omega_0\tau_0$, then

$$q^*(0)=D\left(1,q_1^*,q_2^*\right),\ q^*(1)=q^*(0)\mathrm{e}^{i\omega_0\tau_0},$$

Thus, from the definition of $G^*(0)$ and the fact that

$$G^*(0)q^*(0)=-i\omega_0\tau_0 q^*(0),$$

we can deduce that

$$q_1^*=\frac{a_{23}\left(a_{11}+i\omega_0\right)-a_{13}a_{21}}{a_{13}\left(a_{22}+i\omega_0\right)-a_{12}a_{23}},\ q_2^*=-\frac{a_{11}+i\omega_0+q_1^*a_{12}}{a_{13}}.$$

In order to satisfy the condition $\left\langle q^*(s),q(\theta)\right\rangle=1$, we need to find the corresponding $D$. Thus, from

$$\begin{aligned}\left\langle q^*(s),q(\theta)\right\rangle&=\bar{q}^*(0)q(0)-\int_{-1}^{0}\int_{\xi=0}^{\theta}\bar{q}^*(\xi-\theta)\mathrm{d}\eta(\theta)q(\xi)\mathrm{d}\xi\\&=\bar{D}\left(1,\bar{q}_1^*,\bar{q}_2^*\right)\left(1,q_1,q_2\right)^{\mathrm{T}}\\&\quad-\int_{-1}^{0}\int_{\xi=0}^{\theta}\bar{D}\left(1,\bar{q}_1^*,\bar{q}_2^*\right)\mathrm{e}^{-i\omega_0\tau_0(\xi-\theta)}\mathrm{d}\eta(\theta)\left(1,q_1,q_2\right)^{\mathrm{T}}\mathrm{e}^{i\omega_0\tau_0\xi}\mathrm{d}\xi\\&=\bar{D}\left[1+\bar{q}_1^*q_1+\bar{q}_2^*q_2-\tau_0\bar{q}_2^*\left(a_{34}q_1+a_{35}q_2\right)\mathrm{e}^{-i\omega_0\tau_0}\right]\\&=1,\end{aligned}$$

we can obtain

$$\bar{D}=\frac{1}{1+\bar{q}_1^*q_1+\bar{q}_2^*q_2-\tau_0\bar{q}_2^*\left(a_{34}q_1+a_{35}q_2\right)\mathrm{e}^{-i\omega_0\tau_0}}.$$

Next, by following the method in reference [18], we can obtain the relevant coefficients that determine the direction of Hopf bifurcation and the stability of periodic solutions at the positive equilibrium point of the delay system:

$$\begin{aligned}g_{20}&=2\tau_0\bar{D}\left(a_{14}+a_{15}q_1+a_{16}q_2\right)+2\tau_0\bar{D}\bar{q}_1^*\left(a_{24}q_1+a_{25}q_1^2+a_{26}q_1q_2\right)\\&\quad+2\tau_0\bar{D}\bar{q}_2^*\left(a_{36}q_2+a_{37}q_1^2\mathrm{e}^{-2iw_0\tau_0}+a_{38}q_1q_2\mathrm{e}^{-2iw_0\tau_0}\right),\end{aligned}$$

$$\begin{aligned}g_{11}&=\tau_0\bar{D}\left[2a_{14}+a_{15}\left(q_1+\bar{q}_1\right)+a_{16}\left(q_2+\bar{q}_2\right)\right]\\&\quad+\tau_0\bar{D}\bar{q}_1^*\left[a_{24}\left(q_1+\bar{q}_1\right)+a_{25}2q_1\bar{q}_1+a_{26}\left(q_1\bar{q}_2+\bar{q}_1q_2\right)\right]\\&\quad+\tau_0\bar{D}\bar{q}_2^*\left[a_{36}\left(q_2+\bar{q}_2\right)+a_{37}2q_1\bar{q}+a_{38}\left(q_1\bar{q}_2+\bar{q}_1q_2\right)\right],\end{aligned}$$

$$\begin{aligned}g_{02}&=2\tau_0\bar{D}\left(a_{14}+a_{15}\bar{q}_1+a_{16}\bar{q}_2\right)+2\tau_0\bar{D}\bar{q}_1^*\left(a_{24}\bar{q}_1+a_{25}\bar{q}_1^2+a_{26}\bar{q}_1\bar{q}_2\right)\\&\quad+2\tau_0\bar{D}\bar{q}_2^*\left(a_{36}\bar{q}_2+a_{37}\bar{q}_1^2\mathrm{e}^{2iw_0\tau_0}+a_{38}\bar{q}_1\bar{q}_2\mathrm{e}^{2iw_0\tau_0}\right),\end{aligned}$$

$$\begin{aligned}g_{21}&=\tau_0\bar{D}a_{14}\left(W_{20}^{(1)}(0)+2W_{11}^{(1)}(0)\right)\\&\quad+\tau_0\bar{D}a_{15}\left(W_{11}^{(2)}(0)+\frac{W_{20}^{(2)}(0)}{2}+\bar{q}_1\frac{W_{20}^{(1)}(0)}{2}+q_1W_{11}^{(1)}(0)\right)\\&\quad+\tau_0\bar{D}a_{16}\left(W_{11}^{(3)}(0)+\frac{W_{20}^{(3)}(0)}{2}+\bar{q}_2\frac{W_{20}^{(1)}(0)}{2}+q_2W_{11}^{(1)}(0)\right)\end{aligned}$$

$$
\begin{aligned}
&+\tau_0\bar{D}\bar{q}_1^* a_{24}\left(W_{11}^{(2)}(0)+\frac{W_{20}^{(2)}(0)}{2}+\bar{q}_1\frac{W_{20}^{(1)}(0)}{2}+q_1W_{11}^{(1)}(0)\right)\\
&+\tau_0\bar{D}\bar{q}_1^* a_{25}\left(2W_{11}^{(2)}(0)+\bar{q}_1W_{20}^{(2)}(0)\right)\\
&+\tau_0\bar{D}\bar{q}_1^* a_{26}\left(q_1W_{11}^{(3)}(0)+\bar{q}_1\frac{W_{20}^{(3)}(0)}{2}+\bar{q}_2\frac{W_{20}^{(2)}(0)}{2}+q_2W_{11}^{(2)}(0)\right)\\
&+\tau_0\bar{D}\bar{q}_2^* a_{36}\left(W_{11}^{(3)}(0)+\frac{W_{20}^{(3)}(0)}{2}+\bar{q}_2\frac{W_{20}^{(1)}(0)}{2}+q_2W_{11}^{(1)}(0)\right)\\
&+\tau_0\bar{D}\bar{q}_2^* a_{37}\left(2q_1\mathrm{e}^{-iw_0\tau_0}W_{11}^{(2)}(-1)+\bar{q}_1W_{20}^{(2)}(-1)\mathrm{e}^{iw_0\tau_0}\right)\\
&+\tau_0\bar{D}\bar{q}_2^* a_{38}\left(q_1W_{11}^{(3)}(-1)\mathrm{e}^{-iw_0\tau_0}+\bar{q}_1\frac{W_{20}^{(3)}(-1)}{2}\mathrm{e}^{iw_0\tau_0}\right)\\
&+\tau_0\bar{D}\bar{q}_2^* a_{38}\left(\bar{q}_2\frac{W_{20}^{(2)}(-1)}{2}\mathrm{e}^{iw_0\tau_0}+q_2W_{11}^{(2)}(-1)\mathrm{e}^{-iw_0\tau_0}\right).
\end{aligned}
$$

where

$$
W_{20}(\theta)=\frac{ig_{20}}{\omega_0\tau_0}q(0)\mathrm{e}^{i\omega_0\tau_0\theta}+\frac{\bar{g}_{02}}{3\omega_0\tau_0}\bar{q}(0)\mathrm{e}^{-i\omega_0\tau_0\theta}+E_1\mathrm{e}^{2i\omega_0\tau_0\theta},
$$

$$
W_{11}(\theta)=-\frac{ig_{11}}{\omega_0\tau_0}q(0)\mathrm{e}^{i\omega_0\tau_0\theta}+\frac{\bar{g}_{11}}{\omega_0\tau_0}\bar{q}(0)\mathrm{e}^{-i\omega_0\tau_0\theta}+E_2,
$$

with

$$
E_1=2\begin{pmatrix}2i\omega_0-a_{11} & -a_{12} & -a_{13}\\ -a_{21} & 2i\omega_0-a_{22} & -a_{23}\\ -a_{31} & -a_{34}\mathrm{e}^{-2i\omega_0\tau_0} & 2i\omega_0-a_{33}-a_{35}\mathrm{e}^{-2i\omega_0\tau_0}\end{pmatrix}^{-1}\begin{pmatrix}E_{11}\\ E_{21}\\ E_{31}\end{pmatrix},
$$

$$
E_2=\begin{pmatrix}-a_{11} & -a_{12} & -a_{13}\\ -a_{21} & -a_{22} & -a_{23}\\ -a_{31} & -a_{34} & -a_{33}-a_{35}\end{pmatrix}^{-1}\begin{pmatrix}E_{12}\\ E_{22}\\ E_{32}\end{pmatrix}.
$$

Building upon the preceding analysis and the expressions for $g_{20}$, $g_{11}$, $g_{02}$, and $g_{21}$, we compute the following critical quantities:

$$
c_1(0)=\frac{i}{2\omega_0\tau_0}\left(g_{20}g_{11}-2|g_{11}|^2-\frac{|g_{02}|^2}{3}\right)+\frac{g_{21}}{2},\ \mu_2=-\frac{\mathrm{Re}\{c_1(0)\}}{\mathrm{Re}\{\lambda'(\tau_0)\}},
$$

$$
\beta_2=2\,\mathrm{Re}\{c_1(0)\},\ T_2=-\frac{\mathrm{Im}\{c_1(0)\}+\mu_2\,\mathrm{Im}\{\lambda'(\tau_0)\}}{\omega_0\tau_0},
$$

These parameters govern the nature of the Hopf bifurcation. Concerning the properties of Hopf bifurcations, we state the following theorem:

**Theorem 4.** If $\mu_2>0$ ($\mu_2<0$), a supercritical (subcritical) Hopf bifurcation emerges at $\tau_0$; If $\beta_2<0$ ($\beta_2>0$), the bifurcating periodic solution is asymptotically stable (unstable); If $T_2>0$ ($T_2<0$), the period of the bifurcating periodic solution increases (decreases).

## 5. Numerical Simulation

In this section, we will conduct numerical simulations to verify the correctness of the theoretical results. The initial values are chosen as follows:

$$x(0)=0.41,\ y(0)=0.37,\ z(0)=0.6.$$

Taking parameters

$$a=0.4,\alpha=0.5,\beta=1,b_1=3,b_2=4,c=3,p=0.5,\mu=0.9,$$

the system has a unique positive equilibrium point $E_*(0.3813,0.2122,0.5338)$ at this time, and it is calculated that $\tau_0=2.1558$.

1) When $\tau=0$, the unique positive equilibrium point $E_*$ of system (2) is locally asymptotically stable. The time series diagram and trajectory diagram of system (2) at this time are shown in Figure 1.

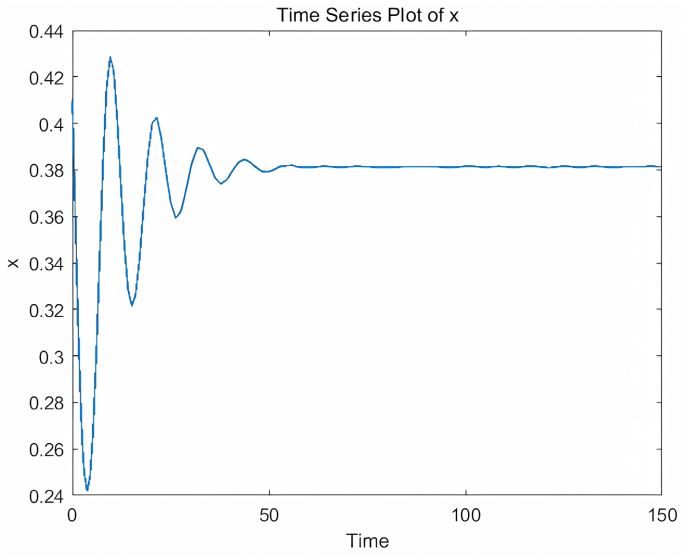


(a)

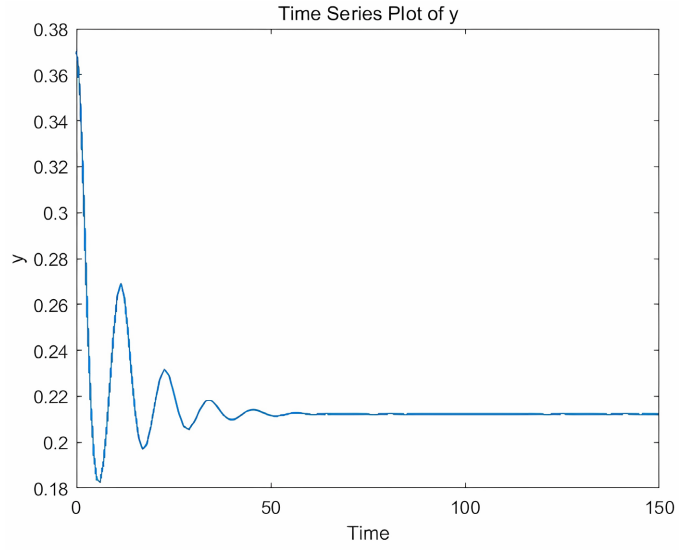


(b)

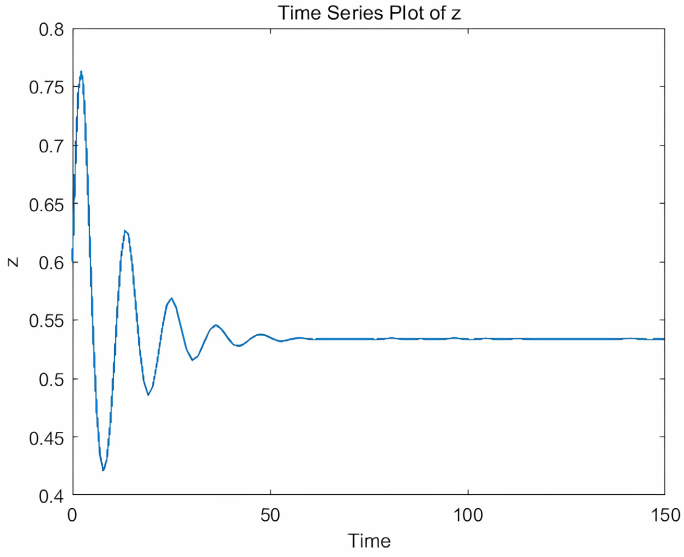


(c)

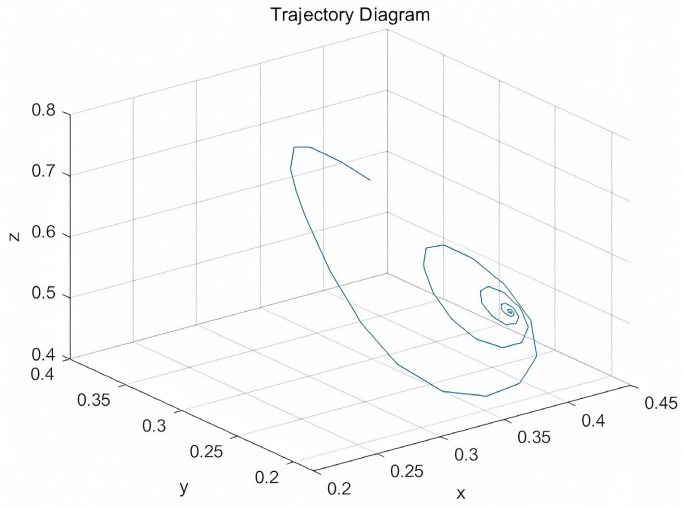


(d)

**Figure 1.** The dynamic behavior of the positive equilibrium point of system (2) in a stable state when $\tau = 0$. (a), (b), and (c) are respectively the time-series diagrams of $x(t)$, $y(t)$ and $z(t)$ when $\tau = 0$. (d) is the trajectory diagram when the positive equilibrium point of system (2) is locally asymptotically stable when $\tau = 0$.

From **Figure 1**, it can be seen that when the gestation delay of the predator $\tau = 0$, under certain parameter values, the positive equilibrium point of the system is in a state of local asymptotic stability. The population quantities of the shared prey, the prey within the guild, and the predator eventually tend to a stable level with the evolution of time. This reflects that without the interference of predator delay, the ecosystem can achieve dynamic population balance through interspecific interactions based on niche differentiation (such as predation, resource competition, and transformation), demonstrating the ecosystem's ability of self-regulation to maintain a steady state. It also provides a non-delayed benchmark

stable state reference for the subsequent exploration of the impact of introducing time delay on ecosystem dynamics, helping to analyze the mechanism by which time delay breaks the balance.

2) To clearly observe the influence of the time delay $\tau$ on the solutions of system (2), a bifurcation diagram of system (2) with respect to the time delay $\tau$ is plotted, as shown in **Figure 2**.

It can be seen from **Figure 2** that the time delay $\tau$ has a significant regulatory effect on the dynamics of the solutions of $x(t)$, $y(t)$, and $z(t)$ in system (2). When $\tau$ is in a low range, the steady-state values corresponding to $x(t)$, $y(t)$, and $z(t)$ are relatively stable, reflecting that the system maintains a stable equilibrium under small time delays. As $\tau$ increases (exceeding the critical value), the steady states of each variable show complex bifurcation characteristics, with

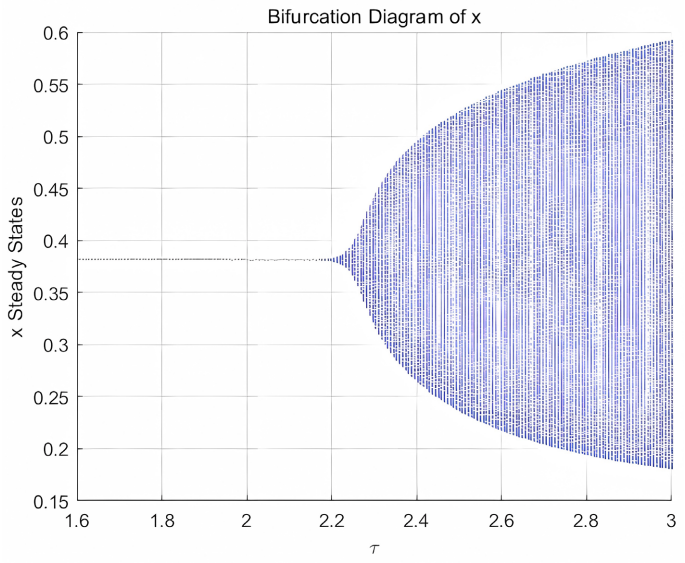


(a)

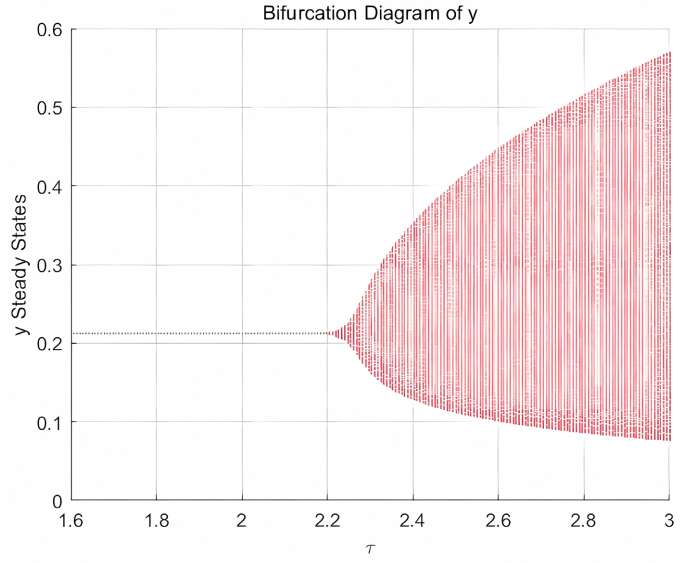


(b)

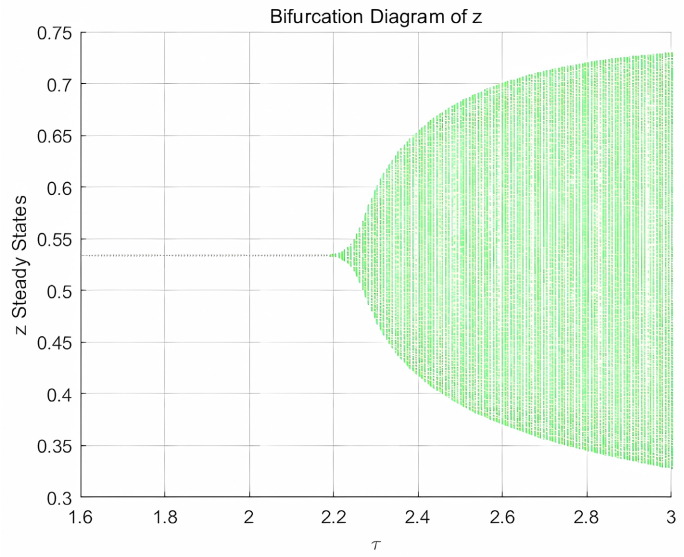


(c)

**Figure 2.** Influence of time delay $\tau$ on the solutions of system (2). (a), (b), and (c) respectively show the influences of time delay $\tau$ on $x(t)$, $y(t)$ and $z(t)$.

the fluctuation range of the solutions expanding and the diversity of states increasing. This indicates that after the time delay exceeds the critical value, the system transitions from a stable equilibrium to periodic oscillations or even more complex dynamics, embodying the nonlinear evolution of ecosystem population dynamics driven by time delay. As a key disturbance factor, time delay changes the time dimension of species interactions, reshapes the stable domain and fluctuation patterns of population quantities, and provides an intuitive basis for analyzing the mechanism of time delay-induced ecosystem instability and dynamic evolution.

3) When $\tau = 1.5 \in [0, \tau_0)$, the time-series diagram and the trajectory diagram of system (2) are shown in **Figure 3**.

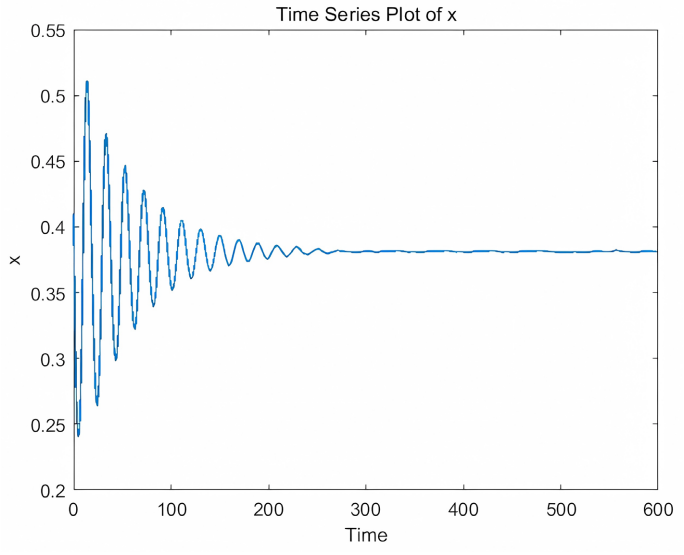


(a)

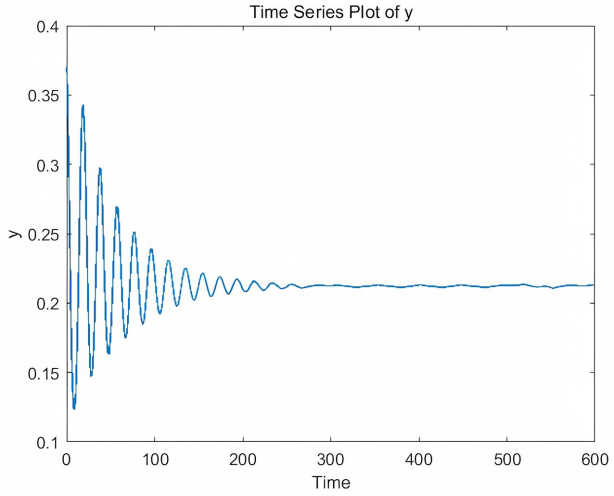


(b)

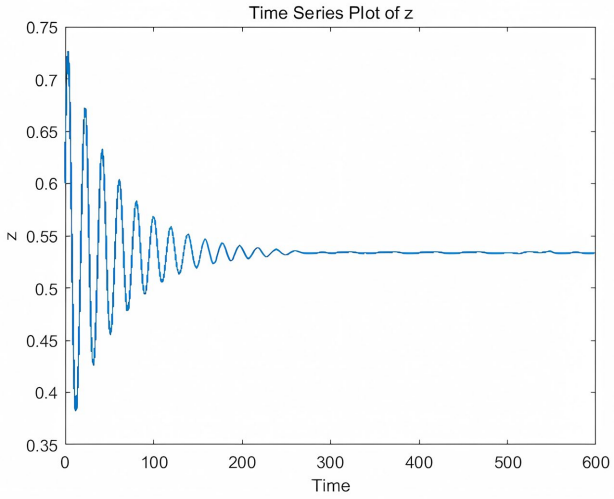


(c)

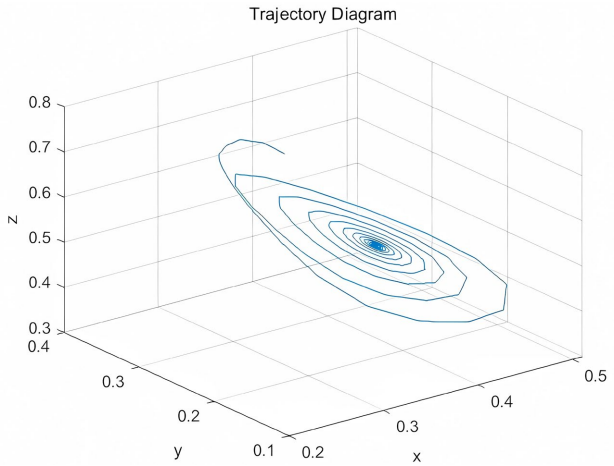


(d)

**Figure 3.** Dynamic behavior of system (2) when $\tau = 1.5$. (a), (b), and (c) are the time-series diagrams of $x(t)$, $y(t)$ and $z(t)$ respectively when $\tau = 1.5$. (d) is the trajectory diagram of system (2) when $\tau = 1.5$.

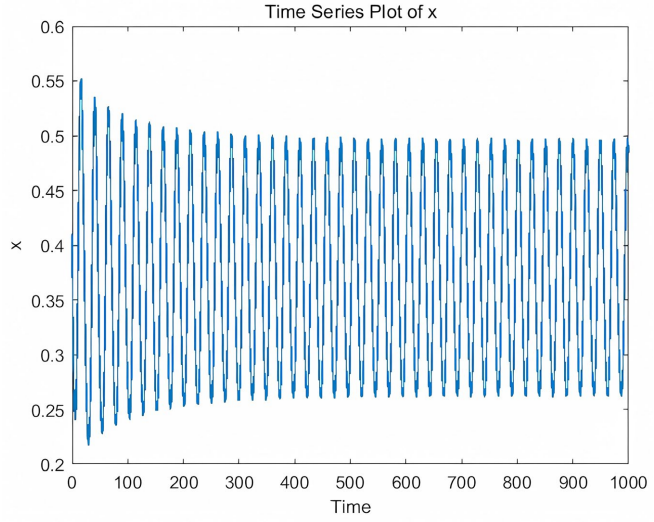
Time Series Plot of x
x
Time
0.6
0.55
0.5
0.45
0.4
0.35
0.3
0.25
0.2
0
100
200
300
400
500
600
700
800
900
1000

(a)

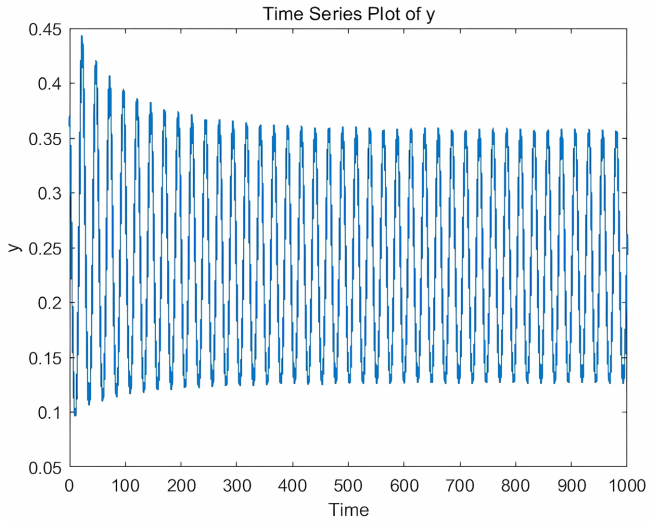
Time Series Plot of y
y
Time
0.45
0.4
0.35
0.3
0.25
0.2
0.15
0.1
0.05
0
100
200
300
400
500
600
700
800
900
1000

(b)

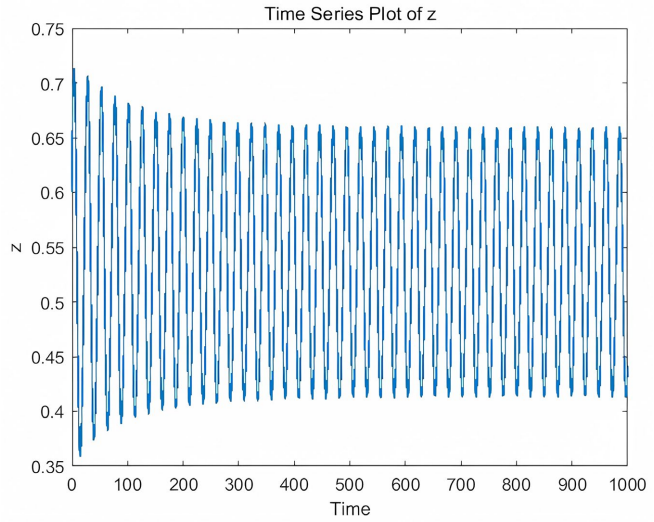
Time Series Plot of z
z
Time
0.75
0.7
0.65
0.6
0.55
0.5
0.45
0.4
0.35
0
100
200
300
400
500
600
700
800
900
1000

(c)

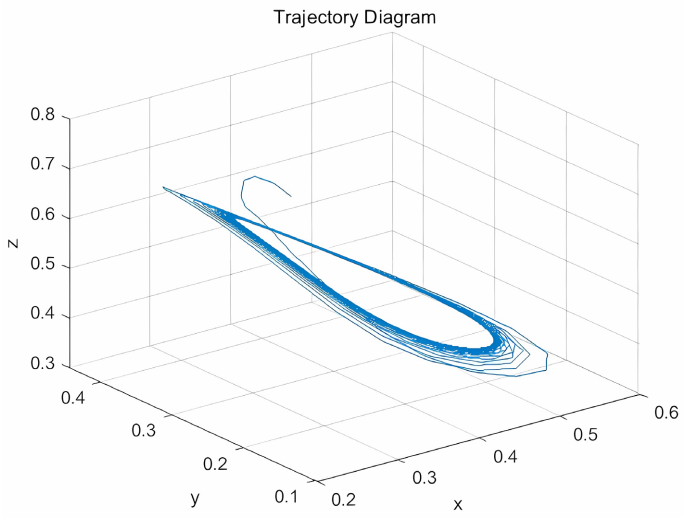


(d)

**Figure 4.** Dynamic behavior of system (2) when $\tau = 2.35$. (a), (b), and (c) are the time-series diagrams of $x(t)$, $y(t)$ and $z(t)$ respectively when $\tau = 2.35$. (d) is the trajectory diagram of system (2) when $\tau = 2.35$.

**Figure 3** and **Figure 4** show that when $\tau$ is small, the time-series diagrams of variables $x(t)$, $y(t)$ and $z(t)$ in system (2) tend to be relatively stable after a short-term fluctuation, and the trajectory diagrams also converge to the center. This indicates that the system is less affected by the time delay at this time and can maintain the dynamic behavior tending to a stable equilibrium. When $\tau$ is large, the time-series of each variable show continuous and regular periodic fluctuations, and the trajectory diagrams form complex closed loops. It shows that after the time delay exceeds the critical value, the system becomes unstable and enters a state of periodic oscillation. This clearly reveals the threshold-regulating effect of the time delay $\tau$ on the system dynamics: under a small time delay $\tau$, the system remains or tends to be stable; when the time delay $\tau$ is large, a Hopf bifurcation is triggered, driving the population dynamics to change from stability to periodic oscillation. This nonlinear dynamic evolution process intuitively depicts the state transition of the ecosystem induced by the time delay, providing a key basis for analyzing the mechanism of population dynamic evolution regulated by the time delay.

4) When $\tau = 2.35 > \tau_0$, the time-series diagram and the trajectory diagram of system (2) are shown in **Figure 4**.

## 6. Conclusions

Based on the niche theory, this study constructs a time-delay IGP (Intraguild Predation) system integrating Holling type I and type II functional responses, and draws the following conclusions through progressive analysis: Firstly, the existence conditions of the positive equilibrium point of the system are clarified, and the establishment conditions of the equilibrium state under niche association are

defined. Secondly, the local stability of the positive equilibrium point in the non-time-delay system is analyzed using the Hurwitz criterion, and the parameter conditions for the stable regulation of populations in the absence of time delay are elaborated. Thirdly, taking the predator's gestation delay as the bifurcation parameter, it is determined whether Hopf bifurcation exists near the positive equilibrium point of the system, the critical point of time delay is derived, and the bifurcation direction and the stability of periodic solutions are analyzed by the center manifold method, revealing the dynamic mechanism of time delay inducing the system to transition from a stable state to periodic oscillation. Finally, numerical simulations are conducted to verify the theoretical results, intuitively presenting the impact of the coupling of time delay and functional responses on population dynamics. However, it should be noted that the current model has certain limitations: it adopts a deterministic framework and does not consider spatial heterogeneity, which may restrict its direct application to real-world ecosystems with stochastic fluctuations and spatial variations.

This study combines single time delay with composite functional responses to analyze the regulatory role of time delay in the IGP system, integrating these two key features into a unified IGP analytical framework on the basis of prior studies that have examined them separately. By investigating their combined effects rather than treating them in isolation, this work thus supplements and extends the existing literature which has predominantly focused on models incorporating only a single functional response or lacking time delay considerations, providing theoretical support for understanding the niche-associated population interactions driven by time delay. The identified stability switch induced by time delay carries important practical implications. For instance, in wildlife management of IGP ecosystems, understanding the critical time delay point where the system shifts from stability to periodic oscillation can inform targeted intervention strategies. Managers could monitor predator gestation periods and adjust conservation measures (such as controlling predator or prey population sizes) to maintain ecosystem stability before the critical delay is reached. This is particularly relevant for conserving keystone species in IGP systems, as periodic oscillations might disrupt species coexistence. Future research can be extended to scenarios with multiple predators and multiple niches, incorporating random disturbances and multiple time delays to construct models that are more consistent with real ecosystems. It is also necessary to further explore the dynamic characteristics of time delay in various interactions such as competition and mutualism, improve the stability criterion system, and promote the in-depth development of ecosystem dynamics theory. In addition, the existing model can be expanded into a double time-delay model to analyze the synergistic mechanism of different time delay sources in the IGP system, explore the transition path of the system from a stable state to complex dynamics (such as chaotic behavior), and provide more effective theoretical tools for biodiversity conservation, population management, and ecological regulation.

## Acknowledgements

The authors are very grateful to Prof. Xiaolin Lin for his valuable suggestions leading to a substantial improvement of the manuscript.

## Conflicts of Interest

The authors declare no conflicts of interest regarding the publication of this paper.

## References

[1] Lotka, A.J. (1925) Elements of Physical Biology. Williams & Wilkins.

[2] Xiao, Y.N., Zhou, Y.C. and Tang, S.Y. (2012) Principles of Biomathematics. Xi'an Jiaotong University Press.

[3] Polis, G.A. and Holt, R.D. (1992) Intraguild Predation: The Dynamics of Complex Trophic Interactions. *Trends in Ecology & Evolution*, **7**, 151-154. https://doi.org/10.1016/0169-5347(92)90208-s

[4] Holt, R.D. and Polis, G.A. (1997) A Theoretical Framework for Intraguild Predation. *The American Naturalist*, **149**, 745-764. https://doi.org/10.1086/286018

[5] Ruggieri, E. and Schreiber, J.S. (2005) The Dynamics of the Schoener-Polis-Holt Model of Intra-Guild Predation. *Mathematical Biosciences and Engineering*, **2**, 279-288. https://doi.org/10.3934/mbe.2005.2.279

[6] Rosenheim, J.A., Kaya, H.K., Ehler, L.E., Marois, J.J. and Jaffee, B.A. (1995) Intraguild Predation among Biological-Control Agents: Theory and Evidence. *Biological Control*, **5**, 303-335. https://doi.org/10.1006/bcon.1995.1038

[7] Arim, M. and Marquet, P.A. (2004) Intraguild Predation: A Widespread Interaction Related to Species Biology. *Ecology Letters*, **7**, 557-564. https://doi.org/10.1111/j.1461-0248.2004.00613.x

[8] Kang, Y. and Wedekin, L. (2012) Dynamics of a Intraguild Predation Model with Generalist or Specialist Predator. *Journal of Mathematical Biology*, **67**, 1227-1259. https://doi.org/10.1007/s00285-012-0584-z

[9] Bai, D., Kang, Y., Ruan, S. and Wang, L. (2021) Dynamics of an Intraguild Predation Food Web Model with Strong Allee Effect in the Basal Prey. *Nonlinear Analysis: Real World Applications*, **58**, Article ID: 103206. https://doi.org/10.1016/j.nonrwa.2020.103206

[10] Liu, Y., Lin, X. and Li, J. (2021) Analysis and Control of a Delayed HIV Infection Model with Cell-to-Cell Transmission and Cytotoxic T Lymphocyte Immune Response. *Mathematical Methods in the Applied Sciences*, **44**, 5767-5786. https://doi.org/10.1002/mma.7147

[11] Liu, W., Lin, X. and Pang, D. (2025) A Delayed Predation Model with Cannibalism and Holling-II Functional Responses. *International Journal of Biomathematics*, 1-26. https://doi.org/10.1142/s1793524525500445

[12] Li, G., Lin, X. and Geng, S. (2025) A Delayed Predator-Prey Model with Fear Effect and Cannibalism. *Journal of Applied Mathematics and Physics*, **13**, 506-524. https://doi.org/10.4236/jamp.2025.132028

[13] Yamaguchi, M., Takeuchi, Y. and Ma, W. (2007) Dynamical Properties of a Stage Structured Three-Species Model with Intra-Guild Predation. *Journal of Computational and Applied Mathematics*, **201**, 327-338. https://doi.org/10.1016/j.cam.2005.12.033

[14] Shu, H., Hu, X., Wang, L. and Watmough, J. (2015) Delay Induced Stability Switch, Multitype Bistability and Chaos in an Intraguild Predation Model. *Journal of Mathematical Biology*, **71**, 1269-1298. https://doi.org/10.1007/s00285-015-0857-4

[15] Han, R. and Dai, B. (2016) Spatiotemporal Dynamics and Hopf Bifurcation in a Delayed Diffusive Intraguild Predation Model with Holling II Functional Response. *International Journal of Bifurcation and Chaos*, **26**, Article ID: 1650197. https://doi.org/10.1142/s0218127416501972

[16] Murdoch, W.W. (1973) The Functional Response of Predators. *Journal of Applied Ecology*, **10**, 335-342.

[17] Holling, C.S. (1959) The Components of Predation as Revealed by a Study of Small-Mammal Predation of the European Pine Sawfly. *The Canadian Entomologist*, **91**, 293-320. https://doi.org/10.4039/ent91293-5

[18] Hassard, B.D. and Kazarinoff, N.D. and Wan, Y.H. (1981) Theory and Applications of Hopf Bifurcation. CUP Archive.